The vertical horopter is not adaptable, but it may be adaptive

Emily A. Cooper Helen Wills Neuroscience Institute, UC Berkeley, USA

Johannes Burge Vision Science Program, UC Berkeley, USA, & Center for Perceptual Systems, Department of Psychology, University of Texas at Austin, USA

Martin S. Banks Vision Science Program, UC Berkeley, USA

Depth estimates from disparity are most precise when the visual input stimulates corresponding retinal points or points close to them. Corresponding points have uncrossed disparities in the upper visual field and crossed disparities in the lower visual field. Due to these disparities, the vertical part of the horopter—the positions in space that stimulate corresponding points—is pitched top-back. Many have suggested that this pitch is advantageous for discriminating depth in the natural environment, particularly relative to the ground. We asked whether the vertical horopter is adaptive (suited for perception of the ground) and adaptable (changeable by experience). Experiment 1 measured the disparities between corresponding points in 28 observers. We confirmed that the horopter is pitched. However, it is also typically convex making it ill-suited for depth perception relative to the ground. Experiment 2 tracked locations of corresponding points while observers wore lenses for 7 days that distorted binocular disparities. We observed no change in the horopter, suggesting that it is not adaptable. We also showed that the horopter is not adaptive for long viewing distances because at such distances uncrossed disparities between corresponding points cannot be stimulated. The vertical horopter seems to be adaptive for perceiving convex, slanted surfaces at short distances.

Keywords: stereopsis, binocular vision, horopter, corresponding points, natural environment, depth perception, cyclovergence

Citation: Cooper, E. A., Burge, J., & Banks, M. S. (2011). The vertical horopter is not adaptable, but it may be adaptive. *Journal of Vision, 11*(3):20, 1–19, http://www.journalofvision.org/content/11/3/20, doi:10.1167/11.3.20.

Introduction

The ground is a prominent feature of the natural environment. It is usually perpendicular to the main axis of the head and body because humans tend to keep themselves aligned with gravity. The pervasiveness of the ground confers a simple relationship between distance and position in the visual field: Near points stimulate the lower field and far points stimulate the upper field. This relationship between environmental structure and position in the visual field yields a systematic pattern of binocular disparities on the retinas: crossed disparity below fixation and uncrossed disparity above fixation (Hibbard & Bouzit, 2005; Potetz & Lee, 2003; Yang & Purves, 2003). It would be useful to take advantage of this regularity when estimating the structure of the environment.

Depth estimates from disparity are most precise when the visual input strikes the retinas on *empirical corresponding points* (Blakemore, 1970). It is useful to describe those points with respect to geometric points. *Geometric corresponding points* are pairs of points with the same coordinates in the two retinas: By definition, they have zero disparity. The two anatomical vertical meridians of the eyes (great circles with zero azimuth) are an example of a set of geometric corresponding points. The locations in the world that stimulate geometric corresponding points define the *geometric horopter*. When fixation is in the head's mid-sagittal plane, the geometric vertical horopter is a vertical line through fixation (Figure 1a). *Empirical corresponding points* are generally defined by determining positions in the two retinas that, when stimulated, yield the same perceived-direction. Empirical and geometric points differ in that empirical points have uncrossed disparities in the upper visual field and crossed disparities in the lower field (i.e., in the upper field, points are offset leftward in the left eye relative to their corresponding points in the right eye; in the lower field, they are offset rightward). This pattern of offsets is often described as a horizontal shear between the empirical corresponding meridians, and this causes the *empirical vertical horopter*—the locus of points in the world that stimulate empirical corresponding points near the vertical meridians—to be pitched top-back (Figure 1b). The qualitative similarity between the disparities of empirical corresponding points and the disparities cast on the retinas by natural scenes has led to the hypothesis that corresponding points are adaptive for precisely perceiving the 3D structure of the natural environment (Breitmeyer, Battaglia, & Bridge, 1977; Helmholtz 1925; Nakayama, 1977).

doi: 10.1167/11.3.20 Received January 31, 2011; published March 28, 2011 ISSN 1534-7362 © ARVO

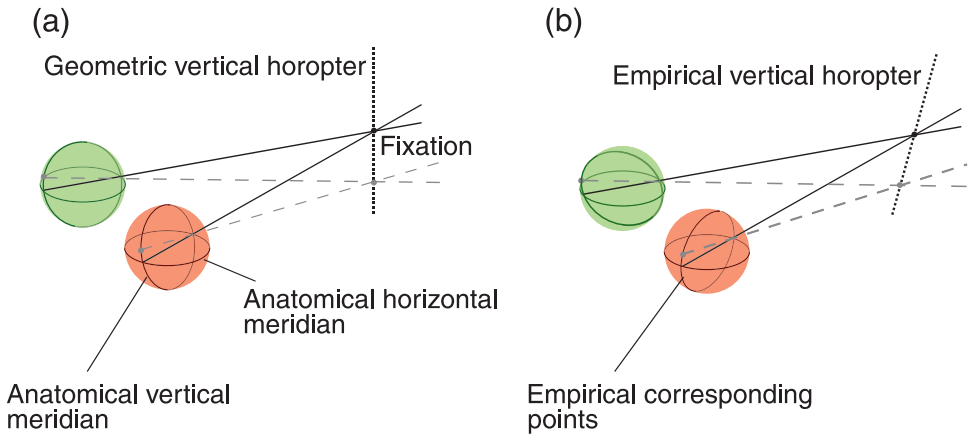

Figure 1. Geometric and empirical vertical horopters. Green and red spheres represent the left and right eyes, respectively. (a) The anatomical vertical meridians of the eyes are geometric corresponding points. When these points are projected into the world, they intersect at a vertical line in the head's mid-sagittal plane (here through fixation): this is the geometric vertical horopter. (b) The empirical vertical horopter has crossed disparity below fixation and uncrossed disparity above fixation, causing a top-back pitch.

The third column of Table 1 (marked θ_v) shows the measured angle between corresponding points near the vertical meridians in all published experiments that used the criterion of equal perceived-direction. The angle is positive in every case, consistent with corresponding points having crossed disparities in the lower visual field and uncrossed disparities in the upper field. However, the measured angle could be a consequence of cyclovergence, the disconjugate rotation of the eyes around the visual axes (Amigo, 1974). Cyclovergence causes equal rotations

Citation	Subject	θ_v (deg)	θ_h (deg)	θ_r ($\theta_v - \theta_h$) (deg)
Helmholtz (1925)	HH[a]	2.66	0.3	2.36
	WV[b]	2.13	–	–
	WV[a]	2.15	–	–
	FS[b]	1.32	–	–
	FS[a]	1.44	–	–
Nakayama (1977)	AC	3.4	0.0	3.4
	CWT	4.8	0.0	4.8
Ledgeway and Rogers (1999)	TL	3.9	0.6	3.3
	BJR	5.8	1.3	4.5
	MLG	2.9	0.5	2.4
Siderov, Harwerth, and Bedell (1999)	AK[1]	0.56	–	–
	AK[2]	0.48	–	–
	HB[1]	0.49	–	–
	HB[2]	0.40	–	–
	LB[1]	0.62	–	–
	LB[2]	0.41	–	–
	MG[1]	0.32	–	–
	MG[2]	0.41	–	–
Grove, Kaneko, and Ono (2001)	PG	1.9	–	–
	HK	1.7	–	–
	NU	1.6	–	–
Schreiber et al. (2008)	PRM	2.8	0.0	2.8
	KMS	6.1	0.0	6.1
	HRF	3.6	0.0	3.6

Table 1. Previous studies of the shear between corresponding points. *Note*: θ_v is the angle between the vertical meridians. θ_h is the angle between the horizontal meridians (cyclovergence). θ_r is the difference between the two, indicating the amount of retinal shear between corresponding points. All of these studies used apparent-motion except: [a]binocular apparent vertical and horizontal; [b]monocular apparent vertical. For Siderov et al. (1999): [1]viewing distance = 200 cm; [2]viewing distance = 50 cm.

between the vertical and horizontal meridians, whereas the hypothesized shear of corresponding points should affect only the horizontal offsets between corresponding points near the vertical meridians. Therefore, to quantify the retinal shear angle, the cyclovergence angle must be subtracted from the measured angle between corresponding points near the vertical meridians. Specifically,

$$\theta_r = \theta_v - \theta_h, \quad (1)$$

where θ_r is the true retinal horizontal shear angle between corresponding points near the vertical meridians, θ_v is the measured angle, and θ_h is cyclovergence. (Obviously, if cyclovergence is zero, the true retinal shear and measured shear are equal.) The last column of Table 1 shows this adjustment for the studies in which both measurements were made. After adjustment, the shear angles are still all positive.

As illustrated in Figure 2, a positive shear between corresponding points near the vertical meridians would make the empirical vertical horopter parallel to the ground plane when an observer's fixation is earth horizontal at infinity. Indeed, the horopter becomes coincident with the ground if the shear angle is

$$\theta_o = 2\tan^{-1}\left(\frac{I}{2h}\right), \quad (2)$$

where I is the observer's inter-ocular distance and h is the observer's eye height. We will call θ_o the *optimal shear angle*. With I = 6.5 cm and h = 160 cm, θ_o = 2.3°

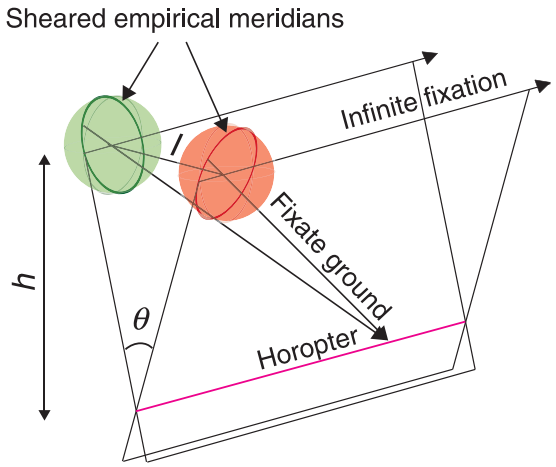

Figure 2. Vertical horopter and the ground. Green and red spheres represent the left and right eyes, respectively. The green and red circles represent the sheared empirical meridians associated with empirical corresponding points. When the eyes are fixated parallel to the ground at infinity, the vertical horopter is a horizontal line extending to meet fixation at infinity. For a given eye height and inter-ocular distance, the optimal shear angle places the horopter in the ground plane. Due to Listing's Law, the horopter remains in the ground when the eyes fixate the ground in the sagittal plane.

(Schreiber, Hillis, Fillipini, Schor, & Banks, 2008). The experimental measurements of the shear angle are reasonably consistent with this optimal value (Table 1). The similarity between observed and optimal shear angles suggests that the vertical horopter may be adaptive for making depth discriminations in the natural environment. Furthermore, for fixations on the ground in the head's sagittal plane, Listing's Law dictates that the horopter will remain coincident with the ground for an observer with an optimal shear value (Helmholtz, 1925; Schreiber et al., 2008). This is also illustrated in Figure 2.

Cats and terrestrial owls are much shorter than humans, so by the above argument their optimal shear angles should be much larger than 2.3° (optimal shear angles for cats and owls are ~10.8° and ~10.6°, respectively). Indeed, physiological data indicate that their shear angles are near these optimal values (Cooper & Pettigrew, 1979), which are consistent with the hypothesis that the shear is adaptive for terrestrial species.

Here, we examine two hypotheses about how the shear angle between corresponding points came to be: the *adaptability hypothesis* and the *hard-coded hypothesis*. The adaptability hypothesis is that an individual's shear angle is determined by his/her experience with the natural environment. According to this hypothesis, corresponding points adapt to optimize precision in depth estimation based on each individual's experience: If experience changes, the shear should change. The hard-coded hypothesis claims that the shear is hard-coded into the visual system because it confers an evolutionary advantage; that is, the shear is adaptive but not adaptable.

We performed a series of experiments to test these two hypotheses. While both hypotheses predict that the average shear angle in the population should be close to the average optimal value, the *adaptability hypothesis* makes the additional prediction that the shear should change with individual experience. We tested this prediction by determining whether observers with different inter-ocular distances and eye heights have different shear angles (Equation 2) and by determining whether an observer's shear angle changes when the experienced patterns of disparities are systematically altered by distorting lenses.

Methods

General methods

In each experiment, we measured the locations of corresponding points using the apparent-motion paradigm of Nakayama (1977). Our primary interest was to determine their locations near the eyes' vertical meridians, but we also measured their locations near the horizontal meridians so that we could subtract any contribution of cyclovergence.

Apparatus

Observers sat 114 cm from a large back-projection screen (61° wide by 51° high) and wore red–green anaglyph glasses. Display resolution was 1280 1024 pixels; each pixel subtended 3 arcmin. Observers were positioned and stabilized with a bite bar such that the midpoint of their inter-ocular axis intersected a surface normal from the center of the screen. The room was dark except for the illuminated screen.

Stimulus and procedure

Observers were instructed to divergently fuse a pair of fixation targets that were presented at eye level and separated by the inter-ocular distance. Fusing these targets produced earth-horizontal fixation at infinity. To measure corresponding points accurately, it is essential to keep eye position constant across trials. The fixation targets were therefore constructed to allow observers to monitor their own fixation. The targets consisted of a radial pattern of 30-arcmin line segments (Schreiber et al., 2008). Some of the segments were presented to the left eye and some to the right (Figure 3a). By assessing the apparent vertical and horizontal alignments of the segments, observers could monitor horizontal and vertical vergences, respectively. We told observers to initiate trials only when the fixation targets were aligned and focused.

For measurements near the vertical meridians, the experimental stimulus consisted of two dichoptic vertical line segments flashed in sequence. The presentation order between eyes was randomized. Each segment subtended 0.75° vertically and 3.4 arcmin horizontally. They were presented for 50 ms, with an inter-stimulus interval of 70 ms (Figure 3b). The line pairs had the same elevation but were displaced horizontally by equal and opposite amounts from the mid-sagittal plane. When the lines fell exactly on corresponding points, observers perceived no horizontal motion; otherwise, they appeared to move leftward or rightward. Line pairs appeared randomly at one of 14 vertical eccentricities from fixation (±2°, 3°, 4°, 5°, 6°, 7°, and 8°). By presenting stimuli at random eccentricities, we greatly reduced the usefulness of anticipatory eye movements. After each trial, observers made a forced-choice judgment of the direction of perceived motion. A 1-up/1-down adaptive staircase varied the horizontal separation between the lines at each eccentricity, with five step-size reductions and 14 reversals. Minimum step size was 1.7 arcmin. Data at each eccentricity were fit with a cumulative Gaussian using a maximum likelihood criterion (Wichmann & Hill, 2001). The mean of the best-fitting cumulative Gaussian (psychometric function) at each eccentricity was defined as the line segment separation that stimulated corresponding points. Figure 4 shows some of these fits for one observer.

The horizontal separations of the points obtained from the Gaussian fits were plotted as a function of eccentricity (Figure 5a). We fit the resulting data with two lines via weighted linear regression. We defined the angle between the vertical meridians (θ_v) as the angle between the best-fit regression lines for the left and right eyes. Azimuth and elevation are plotted in Hess coordinates, a spherical coordinate system in which azimuth and elevation are both measured along major circles (i.e., longitudes). Lines in Cartesian coordinates project to major circles in spherical coordinates, and major circles are plotted as lines in Hess coordinates. Therefore, lines in the world map to lines in Hess coordinates. Using this coordinate system enabled us to readily assess whether the empirical horopter could lie in a plane.

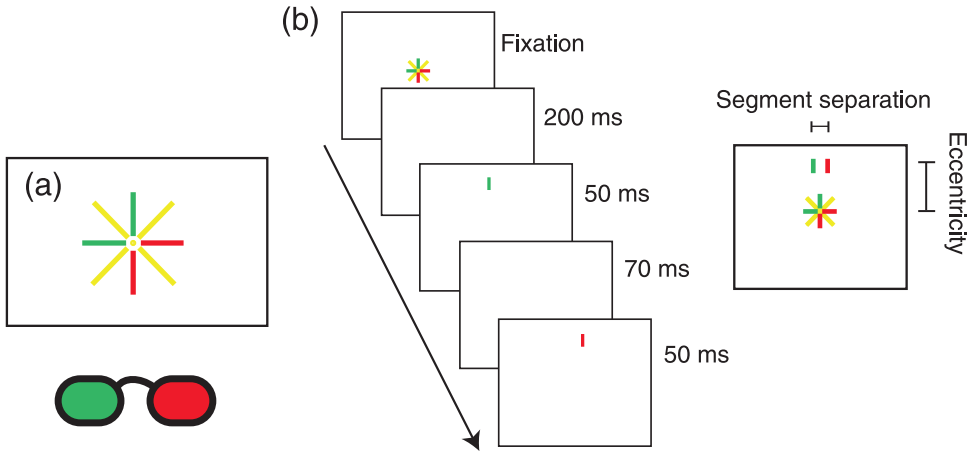

Figure 3. Stimulus and procedure. Observers wore red–green anaglyph glasses. Green, red, and yellow lines represent stimuli seen by the left, right, and both eyes, respectively. (a) The appearance of the fixation target when fused: perceived alignment of dichoptic vertical and horizontal segments indicated accurate horizontal and vertical vergences. Radial bioptic lines aided with maintenance of alignment. (b) Temporal sequence of screens for a trial and the resulting percept integrated over time.

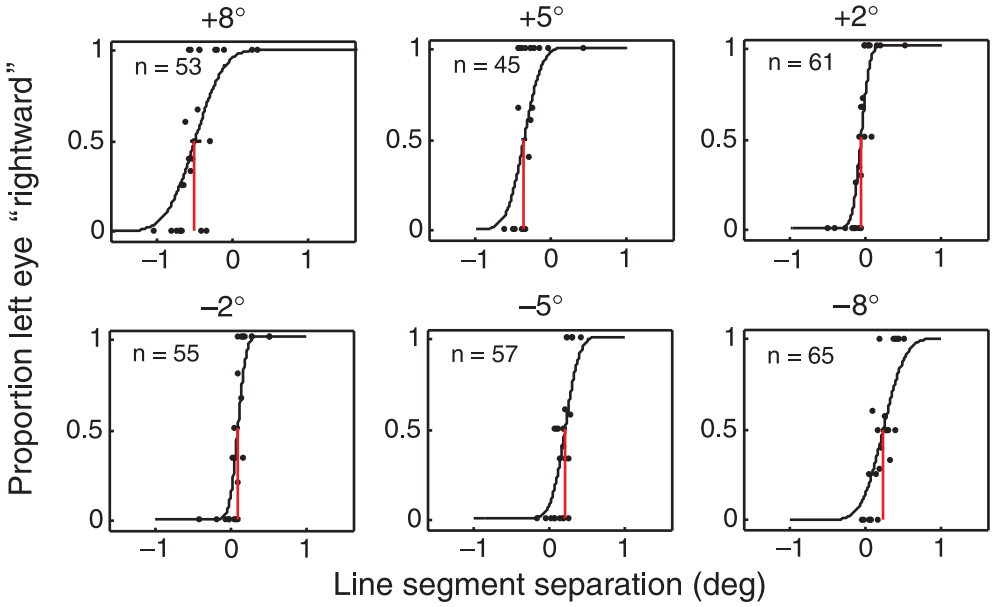

Figure 4. Psychometric functions for observer XMP. Each panel shows the responses for one vertical eccentricity (+8°, +5°, +2°, −2°, −5°, and −8°). The abscissas are the horizontal separation between the lines shown to the left and right eyes. Negative separations indicate uncrossed disparities, and positive separations indicate crossed disparities. The ordinates are the proportion of observer responses indicating that the line presented to the left eye was perceived to the right of the line presented to the right eye (i.e., indicating the lines had crossed disparity). The data were fit with cumulative Gaussians. The means of the Gaussians (indicated by the red vertical lines) were defined as the disparities between corresponding points at each eccentricity.

We measured cyclovergence while observers performed the main experimental task. We did so by presenting dichoptic horizontal line segments near the horizontal meridians. The lines were displaced vertically and observers indicated whether apparent-motion was upward or downward (see Control experiments section for validation of this method). The procedure was otherwise the same as the one we used to estimate corresponding points near the vertical meridians. For these measurements of vertical offsets, 14 additional staircases were randomly interspersed during a session with the other measurements.

Figure 5b plots the separations of line segments near the horizontal meridians that yielded no apparent-motion. We fit these data with regression lines and the angle between these lines was our estimate of cyclovergence. We then used these estimates (θ_h) to correct the measurements near the vertical meridians (θ_v) and thereby obtain an estimate of the retinal shear angle (θ_r; Equation 2). This is shown in Figure 5c.

Experiment 1

In Experiment 1, we measured the horizontal shear angle in observers with different inter-ocular distances and eye heights. The adaptability hypothesis predicts a positive correlation between observers' measured retinal shear (θ_r) and their optimal shear (θ_o from Equation 2). The hard-coded hypothesis predicts no correlation.

Methods

Observers

We recruited 39 observers with a range of optimal shear angles. It was impractical to recruit people based on their inter-ocular distance (most people do not know it), so we recruited people of various heights. Consequently, the population included members of the San Francisco Bay Area Chapter of the Little People of America and members of college basketball and crew teams. Their overall heights ranged from 4.3 to 7.0 ft (129.5 to 213.4 cm).

Eleven observers were excluded because they had reduced stereoacuity, significant exophoria or esophoria, or because they were unable to perform the task (staircases did not converge). One observer was an author; the others were unaware of the experimental hypotheses. All underwent training prior to data collection.

Figure 6a is a scatter plot of inter-ocular distances and eye heights. The two values were not significantly correlated ($r = 0.25$, $p = 0.2$, $df = 26$), so our population had a reasonably wide range of optimal shear angles: 1.5° − 2.8° (mean = 2.1°). Figure 6b is a histogram of these optimal values.

Results

Corresponding points

Figure 7 plots the positions of corresponding points near the vertical meridians for all observers. Offsets due to fixation disparity were first eliminated from the data by shifting the data from the two eyes horizontally until they intersected at zero. Because no measurements were taken at 0° elevation, the amount of shift was determined by finding the x-intercept of a regression line fit to the data (we used quadratic regression lines because much of the data was poorly fit by lines). Rotations due to cyclovergence (θ_h) were also subtracted as shown in Figure 5 (Equation 1). In agreement with the previous literature, all but two observers had corresponding points with uncrossed disparity above fixation and crossed disparity below fixation. (Observer KKD had uncrossed disparity above but no clear pattern of disparity below fixation; LAT had no clear pattern at all.) This means that the vertical horopters of nearly all observers are pitched top-back.

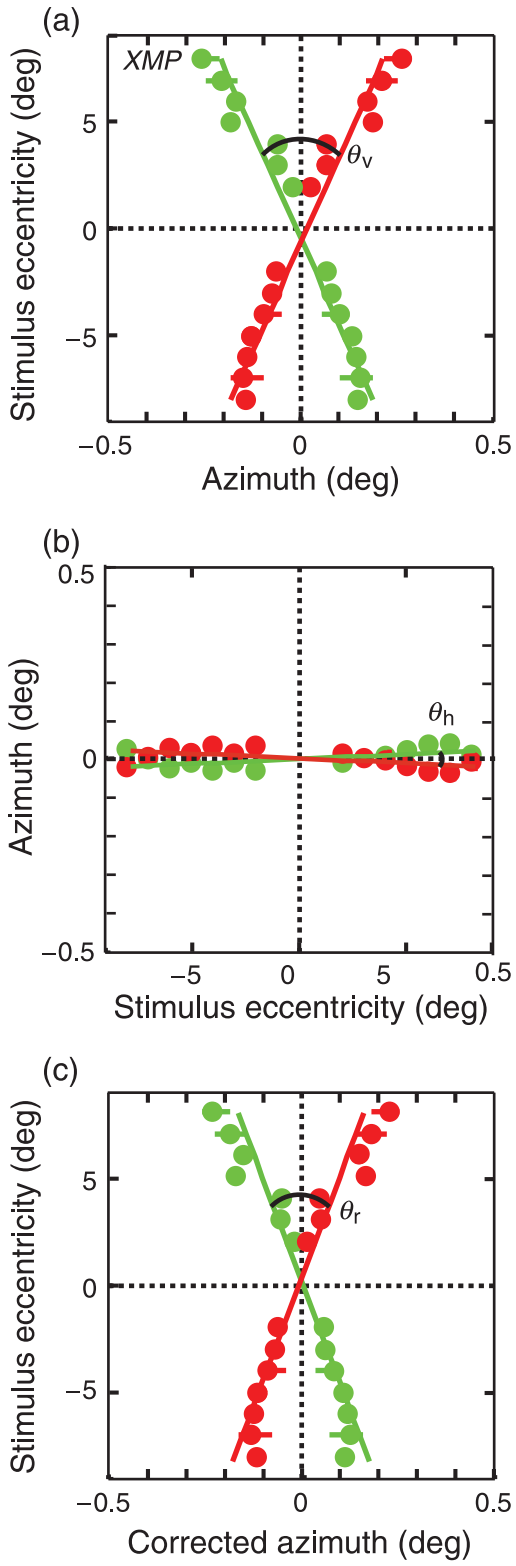

Figure 5. Data from one observer. The data in each panel are plotted in Hess coordinates. (a) Measurements near the vertical meridians before correction for cyclovergence. The abscissa is the horizontal line segment separation for which no motion was perceived. The ordinate is vertical eccentricity. The scale of the abscissa is expanded relative to the scale of the ordinate. At each eccentricity, the green and red dots indicate the measured locations in the left and right eyes, respectively. Error bars represent 95% confidence intervals. The angle between the regression lines is the angle between the measured positions (θ_v). (b) Measured positions of corresponding points near the horizontal meridians. The abscissa is the vertical line separation for which no motion was seen. The ordinate is horizontal eccentricity. The angle (θ_h) is presumed to be due to cyclovergence. (c) Retinal positions of corresponding points near the vertical meridians once corrected for cyclovergence (θ_r; Equation 2).

Retinal shear angle

Figure 8a is a histogram of the measured retinal shear values (θ_r). The mean shear angle was 1.6° and the standard deviation was 0.8°. Figure 8b plots each observer's measured shear value against their optimal shear value. The two values were not significantly correlated ($r(26) = 0.07$, $p = 0.72$). The non-significant correlation between measured and optimal shear suggests that corresponding points are not adjusted to keep the horopter in the ground plane for individuals. This is counter to a prediction of the adaptability hypothesis. However, the average measured value was similar to the average optimal value (2.1°), which is consistent with the hypothesis that the shear is hard-coded to be adaptive for the population in general.

Curvature

In the Hess coordinates we used, lines in the world map to lines in the corresponding point plots. Thus, if the vertical horopter lies in a plane, the data should be well fit by lines. Figure 7 reveals that the data are generally not well fit by lines; this is particularly evident in the far right column.

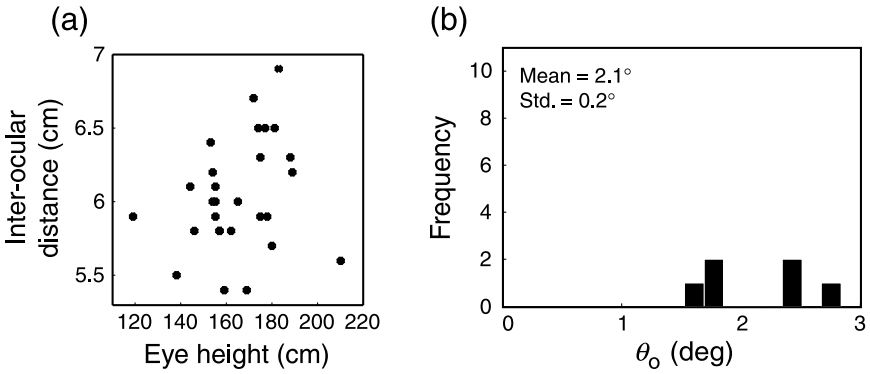

Figure 6. Eye height, inter-ocular distance, and optimal shear (θ_o) angles for the observer population. (a) Scatter plot of eye heights and inter-ocular distances. (b) Histogram showing the distribution of optimal shear angles for the sample population. The mean and standard deviation are shown in the upper left.

These data are best fit by curves with centers that are bent toward zero azimuth. Such convex patterns generate convex vertical horopters (i.e., relative to a slanted line, it is farther from the observer above and below fixation). To illustrate this, Figure 9 shows a side view of the horopter for two observers who are fixating on the ground plane at 0.5 and 1.5 m ahead. Eye position for declined gaze was determined using Listing's Law, so the horopter should be coincident with the ground if the shear is optimal (Equation 2). Observer JAI had a reasonably linear pattern of corresponding points, and the horopter is therefore approximately linear (left panel). Because the shear angle is close to the optimal value, the horopter is also approximately coincident with the ground plane. Observer SEC had a convex pattern of corresponding points, and the horopter is therefore convex and not coincident with the ground (right panel). The prevalence of convex correspondence patterns in our data is thus inconsistent with the original hypothesis that the pattern of corresponding points is an adaptation to the ground plane (Helmholtz, 1925; Schreiber et al., 2008).

To check that the observation of curved correspondence patterns was not caused by a procedural or computational error, we also measured the curvature of corresponding points near the horizontal meridians. Along these meridians, the correspondence pattern should not be curved because non-zero vertical disparities in the apparent-motion task would presumably manifest non-zero cyclovergence. To test this prediction, we compared quadratic regressions of the measurements near the vertical and horizontal meridians for all observers. A two-tailed *t*-test also revealed that the coefficients on the quadratic terms for the fits near the horizontal meridians were not significantly different from zero (mean = 0.001, $df = 26$, $p = 0.496$), which means, as we expected, that there is no curvature in the pattern of correspondence near the horizontal meridians. In contrast, the coefficients for the fits near the vertical meridians were significantly less than zero (mean = −0.009, $df = 26$, $p = 0.004$), consistent with convex horopters.

Experiment 2

In Experiment 1, we observed that the horizontal shears for individual observers were not well correlated with the optimal shears (Equation 2). This result is inconsistent with the adaptability hypothesis. However, our calculation of the optimal shear assumes that the retinal shear is specifically adaptive for the pattern of disparities cast by the ground plane at standing height for fixations in the mid-sagittal plane. Perhaps this specific shear value does not reflect the majority of an observer's experience with disparities in the natural environment. Thus, to further test the adaptability hypothesis, we systematically sheared the disparities delivered to the eyes for seven consecutive days using distorting lenses. If the horopter is adaptable, the shear angle between corresponding points should change in the direction of the shear added by the lenses. If it is hard-coded, no change in shear should occur.

Methods

Observers

Five observers participated. All had corrected-to-normal vision and normal stereoacuity, and all underwent training prior to data collection. Two were authors; the others were unaware of the experimental hypotheses.

Stimulus and procedure

For all waking hours of seven consecutive days, observers wore lenses over the two eyes that systematically

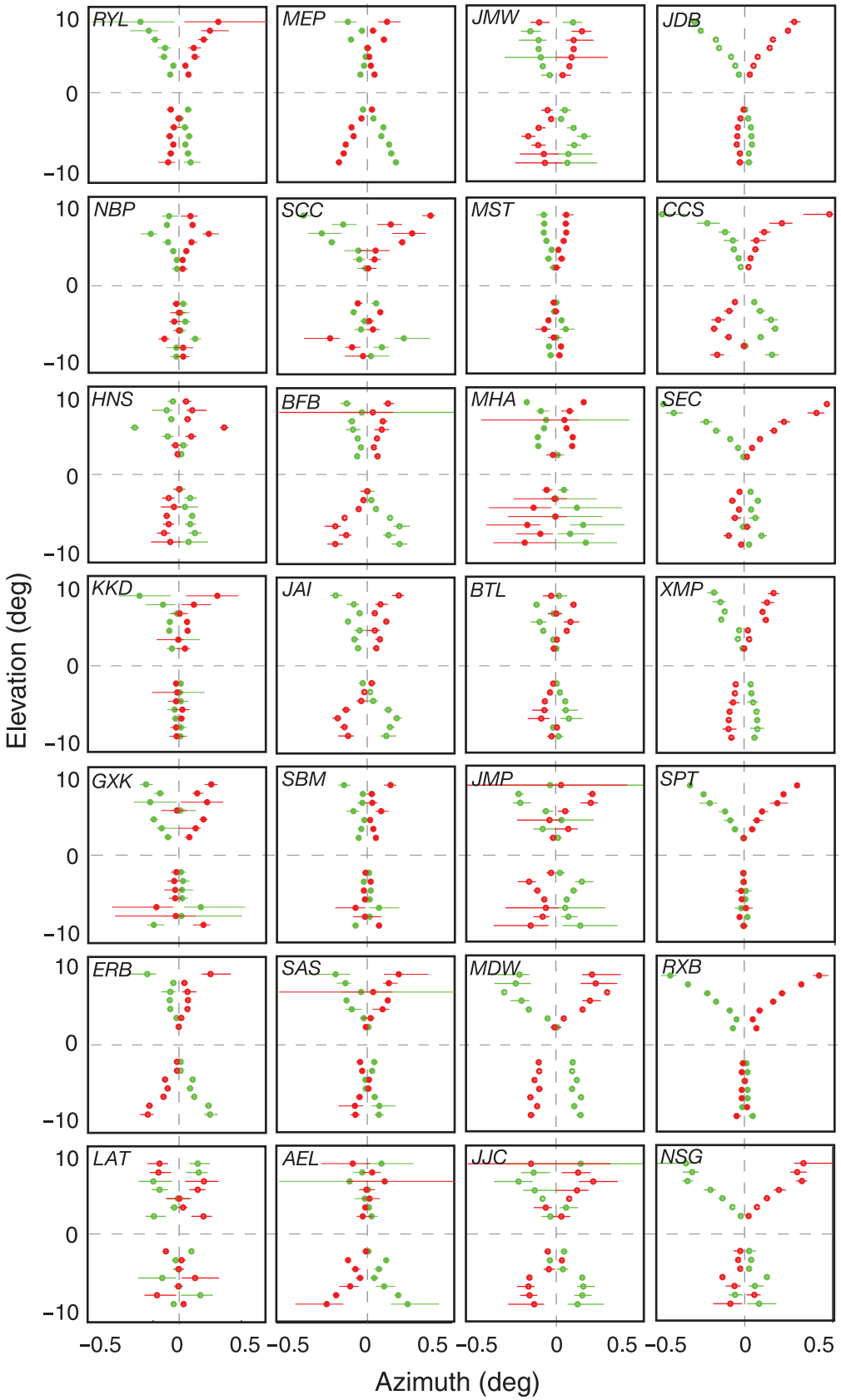

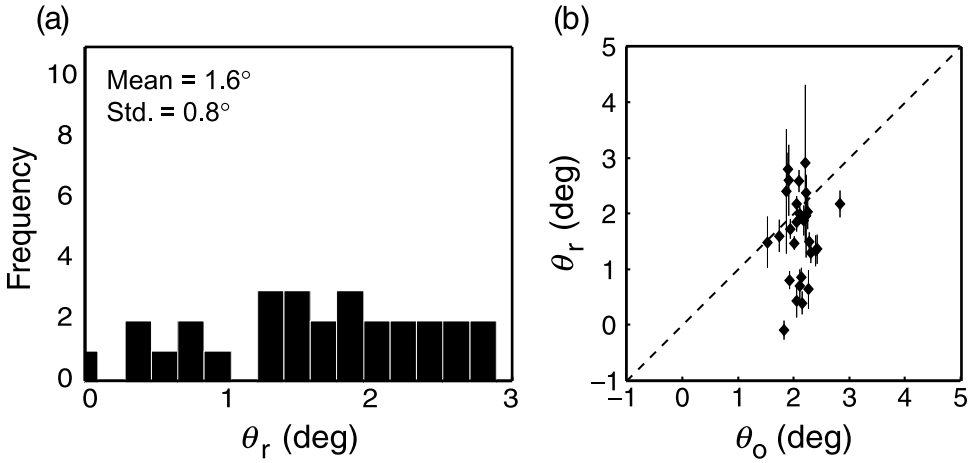

Figure 8. Retinal shear angle in individual observers. (a) Histogram showing distribution of measured retinal shear angles after correction for cyclovergence. The mean and standard deviation are shown in the upper left. (b) Scatter plot of optimal and measured retinal shear angles. The abscissa and ordinate are the optimal and measured angles (again after correction), respectively. Error bars are standard errors, determined by bootstrapping.

altered the pattern of incident disparities. The lenses were afocal unilateral magnifiers (Ogle & Ellerbrock, 1946); they magnify the image along one axis, and not the orthogonal axis, without introducing an astigmatic difference in focal power. The lenses were situated in a frame with their principal axes rotated by ±1.5°. They created equal and opposite shears of the images of a vertical line (±3°), and those shears were opposite to the ones for a horizontal line (±3°). Our goal was to create only a horizontal shearing of vertical lines, but the additional vertical shearing of horizontal lines was a necessary byproduct of creating lenses that did not cause defocus. The overall effect is illustrated in Figure 10.

Three observers wore lenses that created a horizontal shear of +3° (extorsion) and two wore lenses creating a shear of −3° (intorsion). When the lenses were initially put on, frontoparallel surfaces appeared to be pitched top-back (extorting lenses) or top-forward (intorting lenses), as expected from the geometry of the viewing situation (Ogle & Ellerbrock, 1946).

Figure 7. Locations of corresponding points for all observers. The abscissa is the azimuth and the ordinate is the vertical eccentricity. The scale of the abscissa is expanded relative to the scale of the ordinate. The data are plotted in Hess coordinates, a system in which lines in the world map to lines in azimuth–elevation plots. At each eccentricity, the green and red dots indicate the locations of corresponding points in the left and right eyes, respectively. Error bars are 95% confidence intervals for azimuth measurements. Rotations due to cyclovergence (θ_h) and offsets due to fixation disparity were first subtracted from the data. We corrected for fixation disparity by finding the abscissa value at which the regression lines intersected, and then shifting the data horizontally such that the intersection had an ordinate value of zero.

We measured the patterns of corresponding points before, during, and after wearing the lenses. The equipment, stimulus, and procedure were identical to Experiment 1. After an initial training session, subjects came in 24 h prior to putting on the lenses and performed one measurement. There were eight measurements taken during lens wear because one measurement was taken immediately after putting the lenses on, and then measurements were taken at approximately 24-h intervals for the next 7 days. The first post-lens measurement was taken immediately after the lenses were removed on the seventh day and the next measurement was taken 24 h later. As before, we used measurements of vertical disparities near the horizontal meridians to measure cyclovergence and used those measurements to estimate the retinal shear near the vertical meridians.

Results

To determine how much the retinal shear angle (θ_r) changed in response to the distorting lenses, we had to take into account the effects of the optical shear caused by the lenses (because observers wore them during the experimental measurements) and of cyclovergence. To take the optical shear into account, we subtracted the horizontal shear due to the lenses (i.e., +3° or −3°) from the empirical measurements. To take the cyclovergence into account, we subtracted the measured cyclovergence values as in Experiment 1. We found that cyclovergence changed slightly during lens wear: The average increase was 0.5° for observers wearing lenses with ω = +3° and −0.1° for those wearing lenses with ω = −3°. Vertical shear disparity along the horizontal meridians induces cyclovergence (Crone & Everhard-Halm,

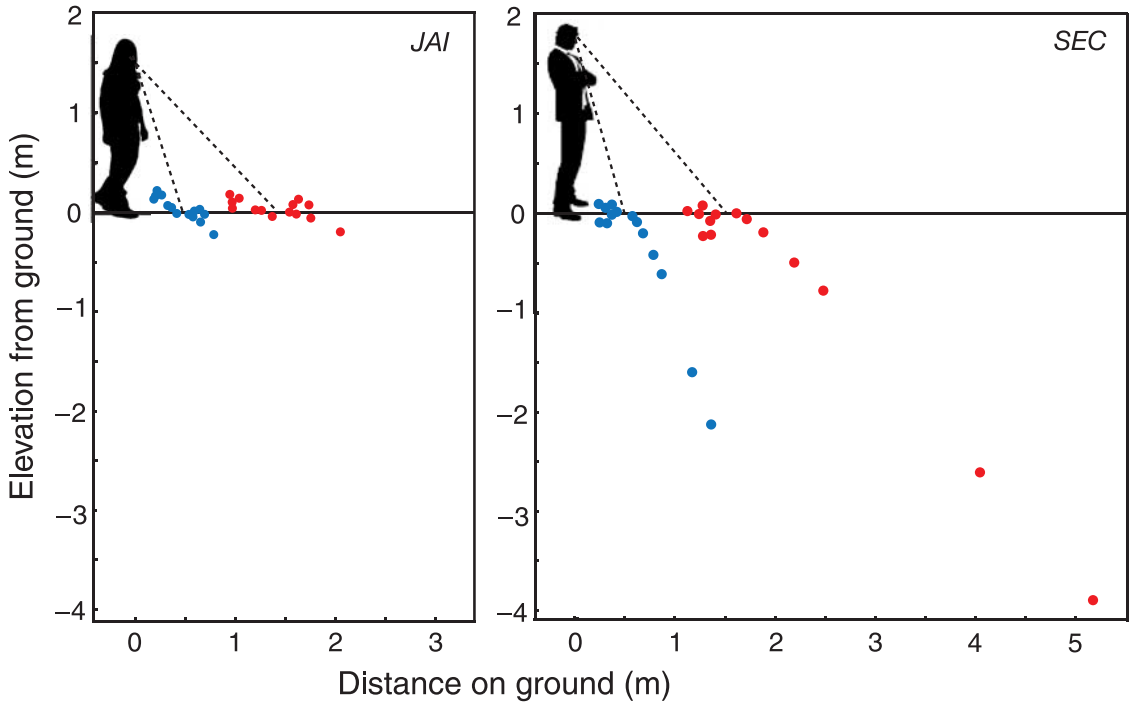

Figure 9. Vertical horopters for two observers. The abscissa is the distance along the ground from the observer's feet. The ordinate is elevation relative to the ground. Two gaze positions are shown with fixation on the ground at 0.5 and 1.5 m in the mid-sagittal plane. In calculating the horopters, eye position was consistent with Listing's Law. (Left) The vertical horopter for observer JAI with linear corresponding point data. This horopter coincides roughly with the ground. (Right) The vertical horopter for SEC with curved corresponding point data. The horopter is convex and therefore not coincident with the ground plane.

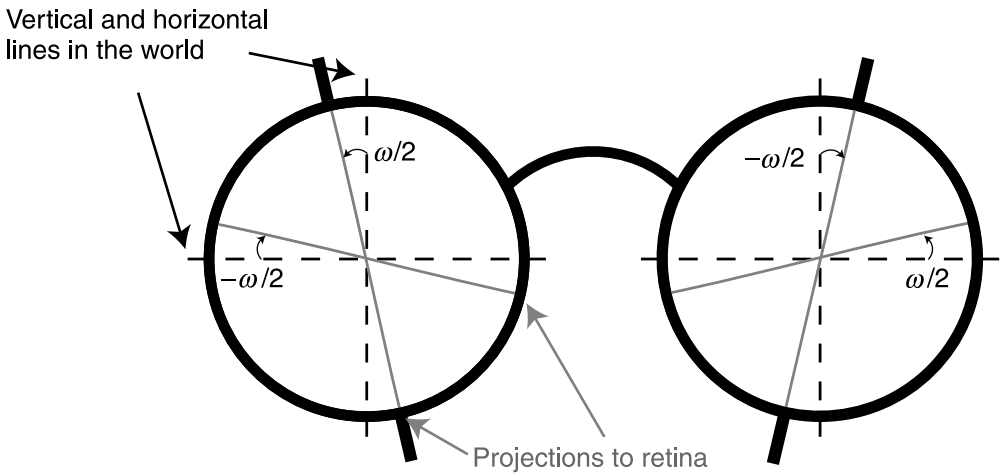

Figure 10. Distorting lenses worn by observers in Experiment 2. Each lens was an afocal unilateral magnifier. The lenses were rotated in opposite directions in the two eyes by $\pm\omega/2°$, creating a horizontal shear disparity of $\omega°$ in the projection of vertical lines. The lenses also created a vertical shear disparity of $-\omega°$ in the projection of horizontal lines.

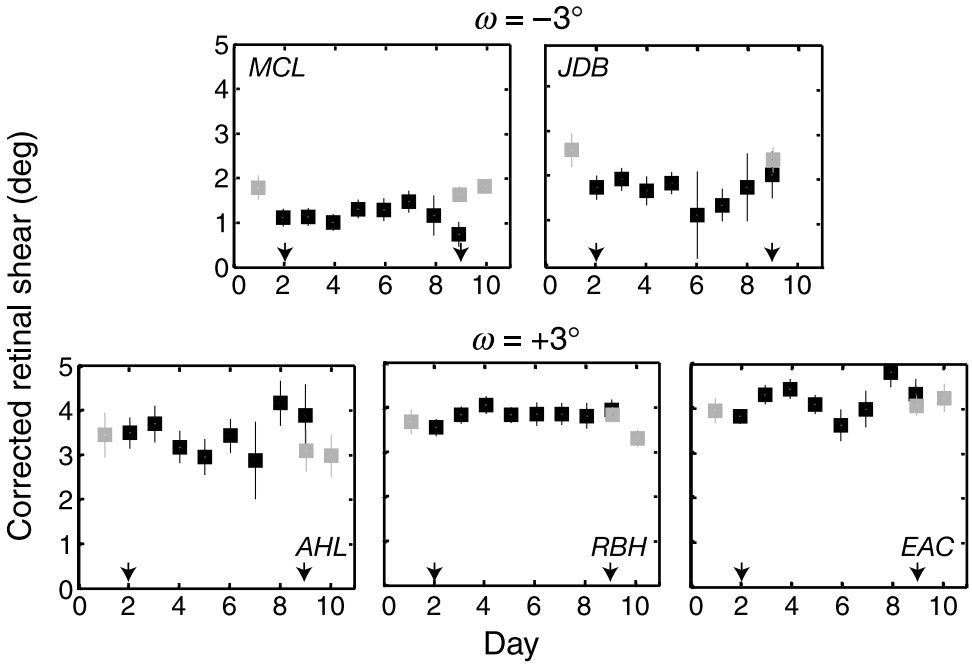

Figure 11. Retinal shear angle before, during, and after wearing the distorting lenses. Corrected retinal shear angle is plotted for each day. The angle has been corrected for cyclovergence and for the shearing effects of the lenses. Thus, the plotted values reflect changes in the retinal positions of corresponding points. One measurement was made before putting the lenses on (gray squares), eight were made while the lenses were on (black squares), and two were made after the lenses were taken off (gray squares). The arrows indicate the days the lenses were first put on and first taken off. Error bars are 95% confidence intervals obtained by bootstrap.

1975), so the change in cyclovergence we observed was surely due to the vertical disparities of the lenses near the horizontal meridians.

Figure 11 shows the corrected retinal shear angle before, during, and after wearing the lenses. There was no systematic change in the retinal shear angle between the vertical meridians for any of the observers. We conclude that corresponding points near the vertical meridians do not adapt in response to a 7-day change in the disparities delivered to the eyes. Consequently, the vertical horopter does not adapt to visual input, at least over the course of a week. This finding, coupled with the observation of no correlation between observer traits (eye height and eye separation) and retinal shear (Figure 8), implies that the vertical horopter is not adaptable.

Despite no change in retinal corresponding points, all five observers experienced perceptual adaptation. They reported that the world appeared distorted when they first wore the lenses (e.g., depending on the sign of ω, frontoparallel surfaces appeared slanted top-back or top-forward, and perceived height was increased or decreased, respectively). However, after 5 days of lens wear, everyone reported that the world appeared undistorted. Four of them also reported perceptual distortions in the opposite direction when the lenses were removed. Closing an eye eliminated the perceptual aftereffect, which suggests that the perceptual effects were due to changes in the interpretation of binocular information and not due to changes in monocular shape representation. However, additional tests would be necessary to confirm this.

Control experiments

Measuring cyclovergence

We assessed the validity of our method for measuring cyclovergence. This subjective method has been frequently used (Banks, Hooge, & Backus, 2001; Ledgeway & Rogers, 1999; Nakayama, 1977) but rarely compared to an objective measurement (but see Crone & Everhard-Halm, 1975; Howard, Ohmi, & Sun, 1993). To assess validity, we measured cyclovergence in the same observers at the same time using the subjective method and an objective measurement of eye position.

Methods

Four observers participated; all were unaware of the experimental hypotheses. They performed the subjective task (described earlier) while the torsional position of both eyes was measured using an eye tracker. Stimuli were projected on 70° 70° screen 100 cm from the midpoint

of the inter-ocular axis. Pixels subtended 3.5 arcmin. The eye tracker was an infrared video-oculography system (SensoMotoric Instruments, Teltow, Germany). It captures 60-Hz video of the pupils and irises and determines cyclovergence by measuring the relative rotation of the irises.

At the beginning of each session, observers fixated a dichoptic target that created stable earth-horizontal fixation at infinity. The center of the target was identical to the fixation target used in the previous experiments. A larger stabilizing stimulus was added to aid alignment of the horizontal meridians of the eyes. This stimulus was a pattern of six 40°-long bioptic (identical in both eyes) radial line segments. After fusing this stimulus for 1 min, eye position was recorded and used as the reference position for the eye tracker. Next, the observer's eyes were induced to change cyclovergence. To induce such changes, we presented a pattern of 40°-long horizontal lines that were rotated in opposite directions for the two eyes by ±3°, ±2°, ±1°, and 0° (Crone & Everhard-Halm, 1975). This new stimulus was also viewed for 1 min. We then began the eye tracking and subjective task. To maintain cyclovergence, the inducing stimulus was presented for 3 s between each apparent-motion trial.

We used the data from the eye tracker as the objective measure of cyclovergence and the data from the apparent-motion task as the subjective measure. The time series data from the eye tracker were thresholded by dropping measurements with reliabilities less than 75%. These reliabilities are calculated automatically by the eye tracker for each time point and reflect the agreement between the current image of the iris and the initial calibration image (Pansell, Schworm, & Ygge, 2003). Time stamps from the eye tracker and the apparent-motion stimulus were used to select the eye-tracking data obtained within ±100 ms of the middle of each apparent-motion trial. Only eye-tracking data obtained within these time windows were included for analysis. The apparent-motion data were analyzed as before to obtain the subjective measure of cyclovergence.

Results

Figure 12 plots the objective and subjective estimates of cyclovergence as a function of the rotation of the cyclovergence stimulus. Each panel shows an individual observer's data. The agreement between the two measures was excellent, which validates the subjective method for measuring cyclovergence.

Cyclovergence in natural viewing

We were concerned about how to properly correct for cyclovergence when estimating the shear angle between corresponding points. Previous studies subtracted cyclovergence from the measured shear in order to estimate the retinal shear angle (Equation 1 and Table 1). However, what if cyclovergence under natural viewing conditions—such as gazing at the horizon while standing upright—is not zero? In that case, subtracting cyclovergence would not yield an estimate of the surface that stimulates corresponding points in natural viewing. To do this, we need to know the cyclovergence of the eyes in natural viewing and then subtract that value from the measured shear. To this end, we next measured cyclovergence for upright observers when a binocular stimulus simulating a floor and hallway was present. We then compared that value to the cyclovergence when only a dichoptic fixation target was present (as in Experiments 1 and 2).

Methods

Five of the original 28 observers participated. We measured cyclovergence using the apparent-motion task. As before, fixation was earth horizontal at infinity. In one condition, the only visible stimuli were the dichoptic fixation target and the flashed lines used in the apparent-motion task (Figure 3); the room was otherwise completely dark. In a second condition, we added a random-dot stereogram that simulated the walls and floor of a hallway. The slant of the simulated floor was adjusted

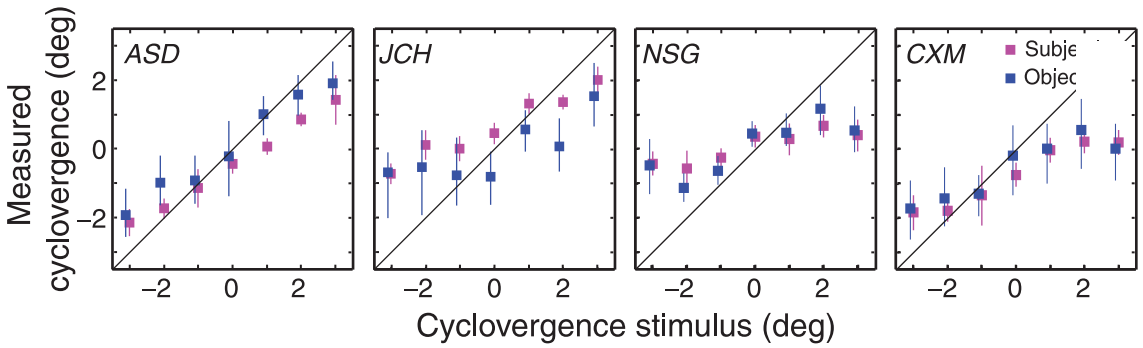

Figure 12. Subjective and objective estimates of cyclovergence. Each panel shows the data from an individual observer. The abscissa is the angular rotation of the inducing lines and the ordinate is the cyclovergence measured with the apparent-motion task (red) and the eye tracker (blue). Error bars are 95% confidence intervals.

for each individual observer to be the same as the slant of a ground plane viewed while standing upright. The conditions were presented in random order.

Results

The average cyclovergence angles in the first (the one with only the fixation target) and second (the one with the floor and walls added) conditions were 0.50° (standard error = 0.14°) and 0.03° (standard error = 0.10°), respectively. These estimates were significantly different (pairwise *t*-test; $df = 8$, $p = 0.01$). They were significantly greater than 0° in the first condition (blank) but not in the second condition (hallway). Assuming that the second condition is more representative of natural viewing than the first condition, these results illustrate the need to measure and correct cyclovergence to zero in Experiments 1 and 2. Thus, our correction procedure was justified.

Discussion

Summary

We found no evidence that the horopter is adaptable: There was no correlation between an observer's eye height/separation and their retinal shear angle and no effect on corresponding point locations after wearing distorting lenses for a week. While null effects can be difficult to interpret, we can conclude that there is no strong effect of experience on the vertical horopter, at least in adults.

We did find that the shear was positive in all but one observer, and that the average shear angle of our observers was similar to the predicted optimal shear angle based on eye height/separation. This is consistent with the hypothesis that the location of the horopter is hard-coded because it is adaptive. However, we also found that many observers had patterns of retinal correspondence that yielded convex horopters. Curved horopters are inconsistent with the hypothesis that the horopter is especially adaptive for making depth discriminations relative to the ground plane. Perhaps the shear is an adaptation to some other common situation in natural viewing.

Convexity

With the exception of Amigo (1974), all previous papers on the vertical horopter have described the deviation of empirical corresponding points from geometric points as a horizontal shear, i.e., horizontal offsets proportional to elevation. We will refer to this correspondence pattern as *linear* because the offsets can be fit with lines. As noted earlier, we observed systematic deviations from linearity in most observers (Figure 7).

It turns out that this deviation has been observed before. Figure 13 plots the data from the three previous studies of the vertical horopter that used the criterion of perceived-direction and that reported data for individual observers. Non-linear correspondence patterns are quite evident in some observers (*PG, PRM, KMS*) and perhaps present in others (*CWT, AC, NU*). Importantly, whenever a deviation from linearity occurs (in our data and theirs), it is always convex (i.e., centers bent toward zero azimuth). Convex patterns of correspondence are evidently common.

In the Hess coordinates we used, convex patterns of corresponding points yield convex vertical horopters. Such horopters cannot be coincident with the ground plane. The observed convexity is thus inconsistent with the theory that the vertical horopter manifests an adaptation for depth perception relative to the ground. Perhaps the horopter is adaptive for a different property of the natural environment.

There is good evidence that the visual system has an expectation, or Bayesian prior, for convex shapes (Langer & Bülthoff, 2001; Liu & Todd, 2004; O'Shea, Agrawala, & Banks, 2010; Sun & Perona, 1998). Such an expectation makes sense because most objects are mostly convex. Perhaps the convexity of the vertical horopter is an adaptation for the most likely shape of surfaces in the natural environment. To evaluate this idea, we need to also examine the shape of the horizontal horopter. The geometric horizontal horopter is the *Vieth–Müller Circle*: the circle containing the fixation point and the nodal points of the eyes. Figure 14a shows a plan view of the geometric horizontal horopter. As shown in Figure 14b, the empirical horizontal horopter is less concave than the geometric horopter, and the *Hering–Hillebrand deviation* (H) quantifies the difference:

$$H = \cot(\alpha_L) - \cot(\alpha_R), \quad (3)$$

where α_L and α_R are the angular locations of corresponding points along the horizontal meridians in the left and right eyes, respectively. Note that the empirical and geometric horizontal horopters are the same when $H = 0$. Table 2 shows the H values reported from several previous studies that used the perceived-direction criterion. H is always greater than zero except for observer *HRF* in Schreiber et al. (2008) and she has intermittent strabismus.

We next compared the shapes of the vertical and horizontal horopters and determined how those shapes changed with viewing distance. For this analysis, we used our measurements of corresponding points near the vertical meridians and data from the literature for corresponding point data near the horizontal meridians (Table 2). First, we calculated average horopters from the vertical and horizontal data. To do this, we found the

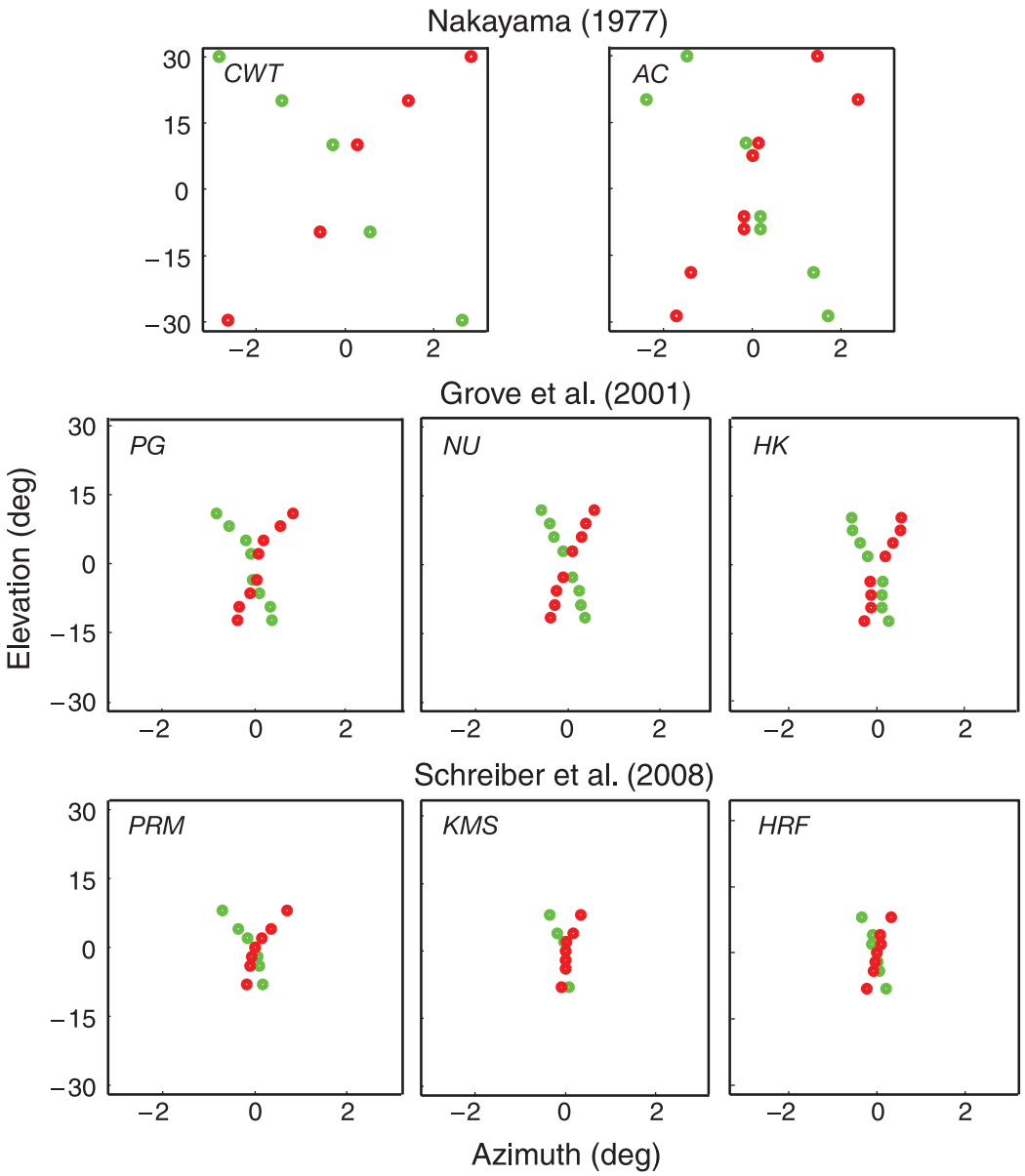

Figure 13. Patterns of corresponding points from previous studies. The data in each panel are plotted in Hess coordinates. The abscissa is the azimuth of the line segments for which no motion is perceived. The ordinate is vertical eccentricity. The scale of the abscissa is expanded relative to that of the ordinate. The green and red dots indicate the measured locations of corresponding points in the left and right eyes, respectively.

average offset between corresponding points at each retinal eccentricity (between −8 and 8°) and determined the locations in space that would stimulate those points. Figure 15a shows top and side views of the average horizontal and vertical horopters, respectively, for three fixation distances (0.5, 1, and 2 m). Fixation is earth horizontal in the mid-sagittal plane. Note that the horizontal horopter is approximately planar at the near distance and becomes increasingly convex at greater distances. The vertical horopter is pitched top-back and is convex at all distances, but the pitch and convexity increase with distance. Next, we quantified the changes in horopter curvature as a function of fixation distance. We plotted each observer's horopter as a function of eccentricity (azimuth for the horizontal horopter and elevation for the vertical). Then, we fit a second-order polynomial to those data and calculated the second derivative ($\partial^2 Z/\partial E^2$). Figure 15b plots the second derivative as a function of fixation distance for the vertical and horizontal horopters. Positive and negative values indicate convex and concave shapes, respectively. Greater magnitudes indicate greater curvature. As expected, the vertical horopter is convex at all distances and becomes increasingly so with increasing distance. The horizontal horopter is concave at near

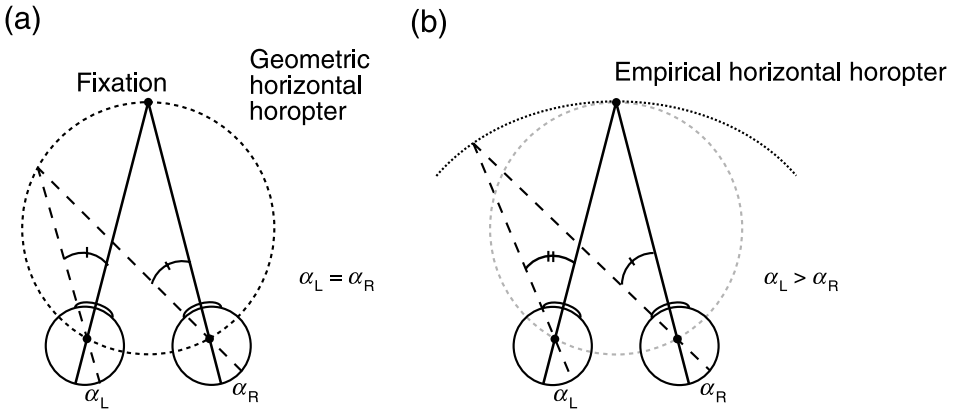

Figure 14. Geometric and empirical horizontal horopters. Circles represent the left and right eyes that are fixating a point in the mid-sagittal plane. (a) Geometric corresponding points along the horizontal meridians have equal horizontal offsets in the eyes: $\alpha_L = \alpha_R$. When these points are projected into the world, they intersect at a circle containing the fixation point and the nodal points of the eyes. This is the geometric horizontal horopter, or Vieth–Müller Circle. (b) Empirical corresponding points along the horizontal meridians have unequal offsets: $\alpha_L > \alpha_R$. This is quantified by the Hering–Hillenbrand deviation (*H*). The deviation is such that the empirical horizontal horopter is less concave than the geometric horopter.

distance (see inset where the second derivative is less than zero), becomes planar at approximately 0.46 m (the abathic distance), and becomes increasingly convex at greater distances. For comparison, we also plot the results of the same analysis for a basketball (men's size 7, radius = 11.8 cm). We used a cross-section of the basketball to determine the osculating circle for a parabola and calculated the second derivative. The basketball is more convex than the horizontal horopter at all plotted distances (at sufficiently great distance, the horopter becomes more convex than the ball). The basketball is more convex than the vertical horopter for distances less than 2 m and less convex than the horopter at greater distances.

This analysis shows that corresponding points are best suited for surfaces that are generally convex and pitched top-back. It would be quite interesting to see if such surfaces are commonplace in natural scenes, particularly surfaces at relative close range where stereopsis is precise.

Subjective measurement of cyclovergence

We estimated cyclovergence in our experiments by measuring the perceived offsets between dichoptic horizontal line segments (i.e., a nonius task). Two previous studies compared subjective (nonius) and objective (eye tracking) estimates of cyclovergence. Howard et al. (1993) compared subjective estimates from vertical nonius lines presented above and below the foveae to objective estimates obtained with scleral search coils. The two estimates did not yield the same values, so they concluded that subjective measurements do not provide an accurate measure of cyclovergence. Crone and Everhard-Halm (1975) compared estimates from horizontal nonius lines slightly above and below the foveae to the locations of ocular blood vessels. They observed close agreement between the two estimates and concluded that subjective methods do allow one to estimate cyclovergence. Unfortunately, Crone and Everhard-Halm made few measurements, so their data were not very convincing.

We propose that the disparity between these two reports stems from the difference in the orientation and location of the nonius lines. The perceived alignment of vertical lines above and below fixation will be affected by both cyclovergence and the shear of retinal corresponding

Paper	Observer	Distance (cm)	*H*
von Liebermann (1910)*		97	0.04
Lau (1921)*		150	0.10
Helmholtz (1925)*		71	0.07
Ogle (1950)	KNO	76	0.08
	AA	76	0.05
	FDC	76	0.05
	WH	60	0.04
Amigo (1967)	PDL	67	0.13
	GA	67	0.07
Hillis and Banks (2001)	MSB	172	0.24
	JMH	172	0.22
	ND	172	0.43
Schreiber et al. (2008)	PRM	40	0.25
	KMS	40	0.36
	HRF	40	−0.11

Table 2. *H* values (Hering–Hillebrand deviation) from previous studies. *Note*: *Values obtained from Ogle (1950). When values were given for various fixation distances, the farthest distance was used.

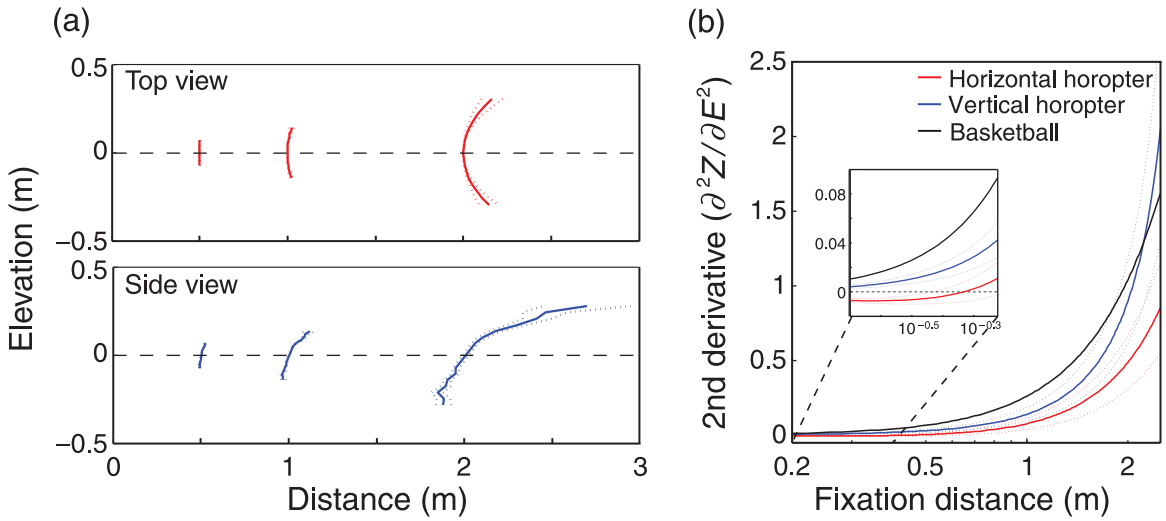

Figure 15. The shapes of the vertical and horizontal horopters as a function of viewing distance. (a) The upper panel is a top view of the empirical horizontal horopter at three fixation distances (0.5, 1, and 2 m). Fixation is earth horizontal in the mid-sagittal plane (gaze direction is indicated by the dashed horizontal lines). In each case, the observer is fixated (that is, converged) where the surface has an ordinate value (distance parallel to inter-ocular axis) of 0. The *H* value (Hering–Hillebrand deviations) used to generate these horopters is 0.13, the average of the values in Table 2. Standard error is indicated by the dotted lines. The lower panel is a side view of the empirical vertical horopter at the same three fixation distances. Again, the observer is fixated where the surface has an ordinate value (distance perpendicular to inter-ocular axis) of 0. The positions of corresponding points used to generate these horopters are the average values across our observers. Standard error is indicated by the dotted lines. (b) Curvature of the vertical and horizontal horopters as a function of fixation distance. The average vertical and horizontal horopters were fit with second-order polynomials. The second derivative of distance as a function of eccentricity ($\partial^2 Z/\partial E^2$), where Z is distance and E is elevation for the vertical horopter and azimuth for the horizontal horopter, of those fitted functions is plotted as a function of fixation distance. The inset is a magnified view of the values for short fixation distances; the ordinate values have been magnified more than the abscissa values. In the main plot and the inset, the values for the horizontal and vertical horopters are indicated by the red and blue curves, respectively. We also used a basketball as an osculating circle to determine a parabola and then computed the second derivative as a function of viewing distance. Those values are indicated by the black curves.

points above and below the foveae. This is not true for horizontal lines near the horizontal meridians because corresponding points in those retinal regions have the same anatomical elevations in the two eyes; as a consequence, perceived misalignment of horizontal lines is caused by cyclovergence alone. The results of our control experiment confirm that horizontal nonius lines presented near the horizontal meridians provide an accurate estimate of cyclovergence across a wide range of eye positions. Thus, horizontal lines to the left and right of fixation should be used when estimating cyclovergence subjectively.

Natural situations in which corresponding points cannot be stimulated

The top-back pitch and curvature of the vertical horopter may be adaptive for short viewing distances, but they are not beneficial for long ones. Here, we show that the pitch and curvature of the horopter preclude the stimulation of corresponding points in the upper visual field at long viewing distances.

In natural viewing, there can never be greater uncrossed disparities than the disparities created by light rays that are parallel to one another (i.e., coming from infinite distance). Because the corresponding points above fixation have uncrossed disparity, there is a fixation distance beyond which those points could never be stimulated by the natural environment. We calculated these critical fixation distances for each retinal eccentricity. In the left panel of Figure 16, a binocular observer fixates a point in the head's mid-sagittal plane at distance Z_0 while a point at distance Z_1 stimulates the retina at locations α_L and α_R relative to the foveae. The horizontal disparity due to Z_1 is the difference in those locations. The horizontal disparity in radians is given by

$$\delta = \frac{(Z_1 - Z_0)I}{Z_1 Z_0}, \tag{4}$$

where I is the inter-ocular separation (Held, Cooper, O'Brien, & Banks, 2010). Rearranging, we obtain

$$Z_1 = \frac{Z_0 I}{I - Z_0 \delta}. \tag{5}$$

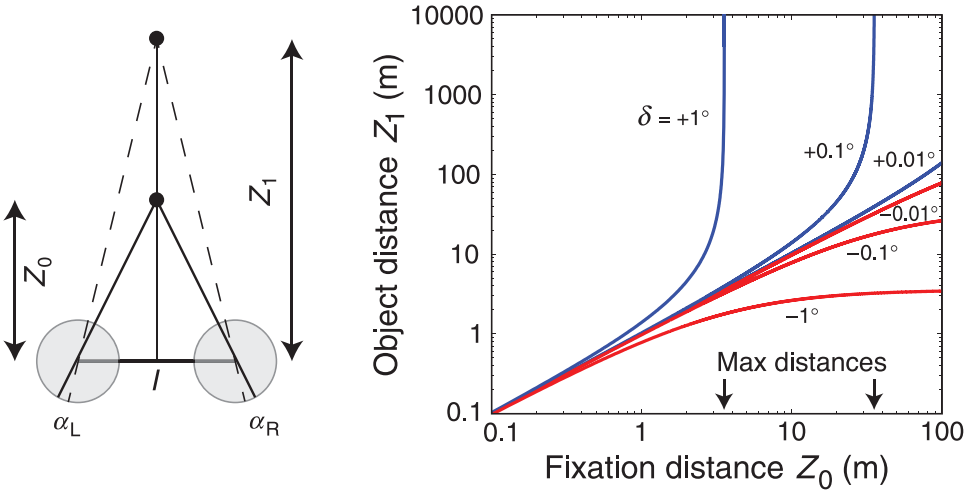

Figure 16. The set of distances that can yield disparities of different values. (Left) The viewing geometry. A binocular observer with inter-ocular distance *I* fixates a point at distance Z_0. Another object at distance Z_1 stimulates the left and right retinas at locations α_L and α_R, respectively, creating horizontal disparity δ. (Right) Given disparity δ, different combinations of fixation and object distance are possible. Object distance Z_1 is plotted as a function of fixation distance Z_0, both in meters. The blue curves are the fixation–object combinations that can occur with positive (uncrossed) disparities and the red curves are the combinations that can occur with negative (crossed) disparities. Each curve is labeled with the specific disparity value, expressed in degrees. We assumed an inter-ocular distance *I* of 0.06 m.

This is the object distance that is associated with a given disparity and fixation distance. Those distances are plotted in the right panel of Figure 16. Blue and red curves correspond to combinations of fixation distances (Z_0) and object distances (Z_1) for positive (uncrossed) disparities and negative (crossed) disparities, respectively; the disparities have been converted to degrees. For each positive disparity, there is a greatest fixation distance Z_0 at which it is possible for that disparity to arise from the natural environment. That greatest distance is I/δ (Equation 5 for $Z_1 = \infty$). For disparities of +0.1° and +1.0°, the greatest fixation distances are 34.4 and 3.44 m, respectively (indicated by arrows in the figure). Greater distances could not possibly give rise to the observed disparity.

Corresponding points nearly always have uncrossed disparity above fixation. The analysis in Figure 16 shows that for each retinal eccentricity, there is a fixation distance beyond which real stimuli cannot stimulate corresponding points. Figure 17 shows those distances as a function of eccentricity in the upper visual field. We conclude there are many natural viewing situations in which corresponding points in the upper visual field cannot possibly be stimulated. (This situation does not generally occur in the lower visual field because corresponding points there almost always have crossed disparity.) Because disparity-based depth discrimination is most precise when corresponding points are stimulated, the precision of depth perception is compromised in such viewing situations.

There are many reasons that stereopsis is not well suited for long viewing distance (Howard & Rogers, 2002). The

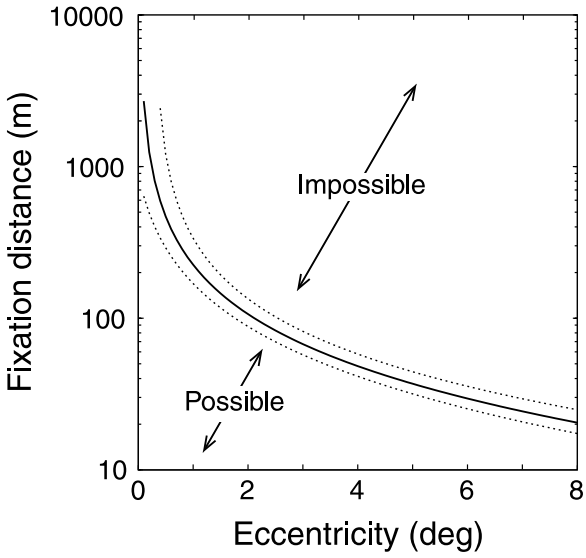

Figure 17. The set of distances and retinal eccentricities for which corresponding points in the upper visual field cannot be stimulated by real stimuli. The critical fixation distance is plotted as a function of eccentricity in the upper visual field. We used the average correspondence pattern across our observers to determine the disparity of corresponding points at each retinal eccentricity. The greatest fixation distance at which such disparity could occur is I/δ, where *I* is inter-ocular distance (assumed to be 0.06 m) and δ is disparity in radians. The dashed lines represent standard errors at each eccentricity calculated from the curves that fit each observer's data. The average correspondence pattern was used to generate this figure. Therefore, the impossible viewing distances apply to the average observer, not necessarily to an individual observer.

fact that real scenes cannot stimulate corresponding points in a large portion of the visual field when the viewer fixates more than a few meters away is yet another.

Acknowledgments

This work was supported by NIH Research Grant EY012851 and NSF Grant BCS-0617701 and by the Department of Defense (DoD) through the National Defense Science and Engineering Graduate Fellowship (NDSEG) Program to EAC. The authors thank Cliff Schor and Jim Maxwell for help with measuring eye movements.

Commercial relationships: none.
Corresponding author: Emily A. Cooper.
Email: emilycooper@berkeley.edu.
Address: 360 Minor Hall, Berkeley, CA 94720, USA.

References

Amigo, G. (1967). The stereoscopic frame of reference in asymmetric convergence of the eyes. *Vision Research, 7,* 785–799.

Amigo, G. (1974). A vertical horopter. *Optica Acta, 21,* 277–292.

Banks, M. S., Hooge, I. T., & Backus, B. T. (2001). Perceiving slant about a horizontal axis from stereopsis. *Journal of Vision, 1*(2):1, 55–79, http://www.journalofvision.org/content/1/2/1, doi:10.1167/1.2.1. [PubMed] [Article]

Blakemore, C. (1970). The range and scope of binocular depth discrimination in man. *The Journal of Physiology, 211,* 599–622. [PubMed]

Breitmeyer, B., Battaglia, F., & Bridge, J. (1977). Existence and implications of a tilted binocular disparity space. *Perception, 6,* 161–164. [PubMed]

Cooper, M. L., & Pettigrew, J. D. (1979). A neurophysiological determination of the vertical horopter in the cat and owl. *Journal of Computational Neurology, 184,* 1–26. [PubMed]

Crone, R. A., & Everhard-Halm, Y. (1975). Optically induced eye torsion: I. Fusional cyclovergence. *Von Graefes Archiv für Klinische und Experimentelle Ophthalmologie, 195,* 231–239.

Grove, P. M., Kaneko, H., & Ono, H. (2001). The backward inclination of a surface defined by empirical corresponding points. *Perception, 30,* 411–429. [PubMed]

Held, R., Cooper, E. A., O'Brien, J., & Banks, M. S. (2010). Using blur to affect perceived distance and size. *ACM Transactions on Graphics, 29,* 1–16.

Helmholtz, H. (1925). Treatise on physiological optics. In J. P. C. Southall (Ed.), (vol. III, pp. 1–688.). New York: Dover. (Original work published 1866)

Hibbard, P. B., & Bouzit, S. (2005). Stereoscopic correspondence for ambiguous targets is affected by elevation and fixation distance. *Spatial Vision, 18,* 399–411. [PubMed]

Hillis, J. M., & Banks, M. S. (2001). Are corresponding points fixed? *Vision Research, 41,* 2457–2473. [PubMed]

Howard, I. P., Ohmi, M., & Sun, L. (1993). Cyclovergence: A comparison of objective and psychophysical measurements. *Experimental Brain Research, 97,* 349–355. [PubMed]

Howard, I. P., & Rogers, B. J. (2002). *Seeing in depth. Depth perception*. Ontario, Canada: I Porteuous Thornhill.

Langer, M. S., & Bülthoff, H. H. (2001). A prior for global convexity in local shape-from-shading. *Perception, 30,* 403–410. [PubMed]

Lau, E. (1921). Neue Untersuchungen über das Tiefen- und Ebenensehen. *Zeitschrift für Psychologie und Physiologie der Sinnesorgane Abteilung, 53,* 1–35.

Ledgeway, T., & Rogers, B. J. (1999). The effects of eccentricity and vergence angle upon the relative tilt of corresponding vertical and horizontal meridian revealed using the minimum motion paradigm. *Perception, 28,* 143–153. [PubMed]

Liu, B., & Todd, J. T. (2004). Perceptual biases in the interpretation of 3D shape from shading. *Vision Research, 44,* 2135–2145. [PubMed]

Nakayama, K. (1977). Human depth perception. *Society of Photo-Optical Instrumentation Engineers Journal, 120,* 2–9.

Ogle, K. N. (1950). *Researches in binocular vision*. Philadelphia: Saunders.

Ogle, K. N., & Ellerbrock, V. J. (1946). Cyclofusional movements. *AMA Archives of Ophthalmology, 36,* 700–735. [PubMed]

O'Shea, J. P., Agrawala, M., & Banks, M. S. (2010). The influence of shape cues on the perception of lighting direction. *Journal of Vision, 10*(12):21, 1–21, http://www.journalofvision.org/content/10/12/21, doi:10.1167/10.12.21. [PubMed] [Article]

Pansell, T., Schworm, U., & Ygge, J. (2003). Torsional and vertical eye movements during head tilt dynamic characteristics. *Investigative Opthalmology & Visual Science, 44,* 2986–2990.

Potetz, B., & Lee, T. S. (2003). Statistical correlations between 2D images and 3D structures in natural scenes. *Journal of the Optical Society of America, 20,* 1292–1303. [PubMed]

Schreiber, K. M., Hillis, J. M., Filippini, H. R., Schor, C. M., & Banks, M. S. (2008). The surface of the empirical horopter. *Journal of Vision, 8*(3):7, 1–20, http://www.journalofvision.org/content/8/3/7, doi:10.1167/8.3.7. [PubMed] [Article]

Siderov, J., Harwerth, R. S., & Bedell, H. E. (1999). Stereopsis, cyclovergence and the backwards tilt of the vertical horopter. *Vision Research, 39,* 1347–1357. [PubMed]

Sun, J., & Perona, P. (1998). Where is the sun? *Nature Neuroscience, 1,* 183–184. [PubMed]

von Liebermann, K. (1910). Beiträge zur Lehre von der binocularen Tiefenlokalization. *Zeitschrift für Psychologie und Physiologie der Sinnesorgane, 44,* 428–443.

Wichmann, F. A., & Hill, N. J. (2001). The psychometric function: I. Fitting, sampling, and goodness of fit. *Perception & Psychophysics, 63,* 1293–1313. [PubMed]

Yang, Z., & Purves, D. (2003). A statistical explanation of visual space. *Nature Neuroscience, 6,* 632–640. [PubMed]